AIP Advances

Structural, electronic transport and magnetoresistance of a 142nm lead telluride nanowire synthesized using stress-induced growth

Dedi, Chia-Hua Chien, Te-Chih Hsiung, Yu-Chieh Chen, Yi-Cheng Huang, Ping-Chung Lee, Chih-Hao Lee, and Yang-Yuan Chen

Citation: AIP Advances **4**, 057111 (2014); doi: 10.1063/1.4876919
View online: http://dx.doi.org/10.1063/1.4876919
View Table of Contents: http://scitation.aip.org/content/aip/journal/adva/4/5?ver=pdfcov
Published by the AIP Publishing

Articles you may be interested in

Stress-induced growth of single-crystalline lead telluride nanowires and their thermoelectric transport properties
Appl. Phys. Lett. **103**, 023115 (2013); 10.1063/1.4813606

Electronic structure of lead telluride-based alloys, doped with vanadium
Low Temp. Phys. **39**, 76 (2013); 10.1063/1.4775748

Atomistic study of electronic structure of PbSe nanowires
Appl. Phys. Lett. **98**, 212105 (2011); 10.1063/1.3592577

Electronic structure of chromium-doped lead telluride-based diluted magnetic semiconductors
Low Temp. Phys. **37**, 210 (2011); 10.1063/1.3573664

High power light emission of IV–VI lead salt multiple-quantum-well structure grown by molecular-beam epitaxy on 111 BaF 2 substrate
Appl. Phys. Lett. **82**, 493 (2003); 10.1063/1.1540238

AIP Publishing Re-register for Table of Content Alerts

Create a profile. Sign up today!

All article content, except where otherwise noted, is licensed under a Creative Commons Attribution 3.0 Unported license. See: http://creativecommons.org/licenses/by/3.0/
Downloaded to IP: 140.109.103.227 On: Wed, 14 May 2014 02:53:04

AIP ADVANCES **4**, 057111 (2014)

Structural, electronic transport and magnetoresistance of a 142nm lead telluride nanowire synthesized using stress-induced growth

Dedi,[1,2,3,4,a] Chia-Hua Chien,[1,2,3] Te-Chih Hsiung,[2,3,5] Yu-Chieh Chen,[2] Yi-Cheng Huang,[2] Ping-Chung Lee,[2] Chih-Hao Lee,[1] and Yang-Yuan Chen[2,a]

[1]*Department of Engineering and System Science, National Tsing Hua University, Hsinchu 30013, Taiwan*
[2]*Institute of Physics, Academia Sinica, Taipei 11529, Taiwan*
[3]*Nano Science and Technology Program, Taiwan International Graduate Program, Institute of Physics, Academia Sinica, Taipei 11529, Taiwan*
[4]*Research Center for Electronics and Telecommunication, Indonesian Institute of Sciences Bandung, Indonesia*
[5]*Department of Physics, National Taiwan University, Taipei 106, Taiwan*

(Received 11 February 2014; accepted 2 May 2014; published online 13 May 2014)

In this study, structurally uniform single crystalline PbTe nanowires (NWs) were synthesized using a stress-induced growth. Selected-area electron diffraction patterns show that the PbTe NWs were grown along the [100] direction. The electrical conductivity σ of a NW with 142 nm in diameter exhibited a semiconducting behavior at 50–300 K. An enhancement of electrical conductivity σ up to 2383 S m^{-1} at 300 K is much higher than σ [0.44–1526 S m^{-1}, Chen *et al.*, Appl. Phys. Lett. **103**, p023115, (2013)] in previous studies. The room temperature magnetoresistance of the 142 nm NW was ∼0.8% at B = 2 T, which is considerably higher than that [0.2% at B = 2 T, Ovsyannikov *et al.*, Sol. State Comm. **126**, 373, (2003)] of the PbTe bulk reported. © *2014 Author(s). All article content, except where otherwise noted, is licensed under a Creative Commons Attribution 3.0 Unported License.* [http://dx.doi.org/10.1063/1.4876919]

I. INTRODUCTION

PbTe is a semiconductor with an energy band gap of 0.32 eV at 300 K. As an $A^{IV}B^{VI}$ narrow-gap semiconductor that acquires new properties when doped, it is suitable for applications in mid-infrared lasers,[1–3] optical detectors,[4,5] and thermoelectricity.[6–8] PbTe doped with transition elements is perspective material for applications in spintronics. Electrical properties in such manner obtained materials strongly depend on the type and concentration of the added dopants.[9] Various phenomena have been observed in doped $A^{IV}B^{VI}$ compounds, which not only show the potential application of the doped semiconductors but also indicate that numerous properties are unique to these compounds.[10] Magnetoresistance (MR) measurements provide an informative technique for characterizing NWs because they yield detailed information about the geometry of the Fermi surface[11,12] and localization effects in the NWs.[13,14] The presence of the peak in the MR of NWs requires a high quality crystal with long mean free paths of carrier along the NW axis, so that most scattering events occur at the wire boundary instead of at a grain boundary, at impurities sites, or at defect sites within the nanowire. We previously synthesized PbTe NWs from a PbTe thin film on a SiO_2/Si substrate using a stress-induced method,[15] the technique provide high-quality single crystals of NWs. Thus these high qualities crystalline NWs are adequate for the study which has not

[a]Authors to whom correspondence should be addressed: E-mail: dediamada@phys.sinica.edu.tw; E-mail: cheny2@phys.sinica.edu.tw; Tel: +886-2-2789-6725; Fax: +886-2-2783-4187

 © Author(s) 2014

All article content, except where otherwise noted, is licensed under a Creative Commons Attribution 3.0 Unported license. See: http://creativecommons.org/licenses/by/3.0/
Downloaded to IP: 140.109.103.227 On: Wed, 14 May 2014 02:53:04

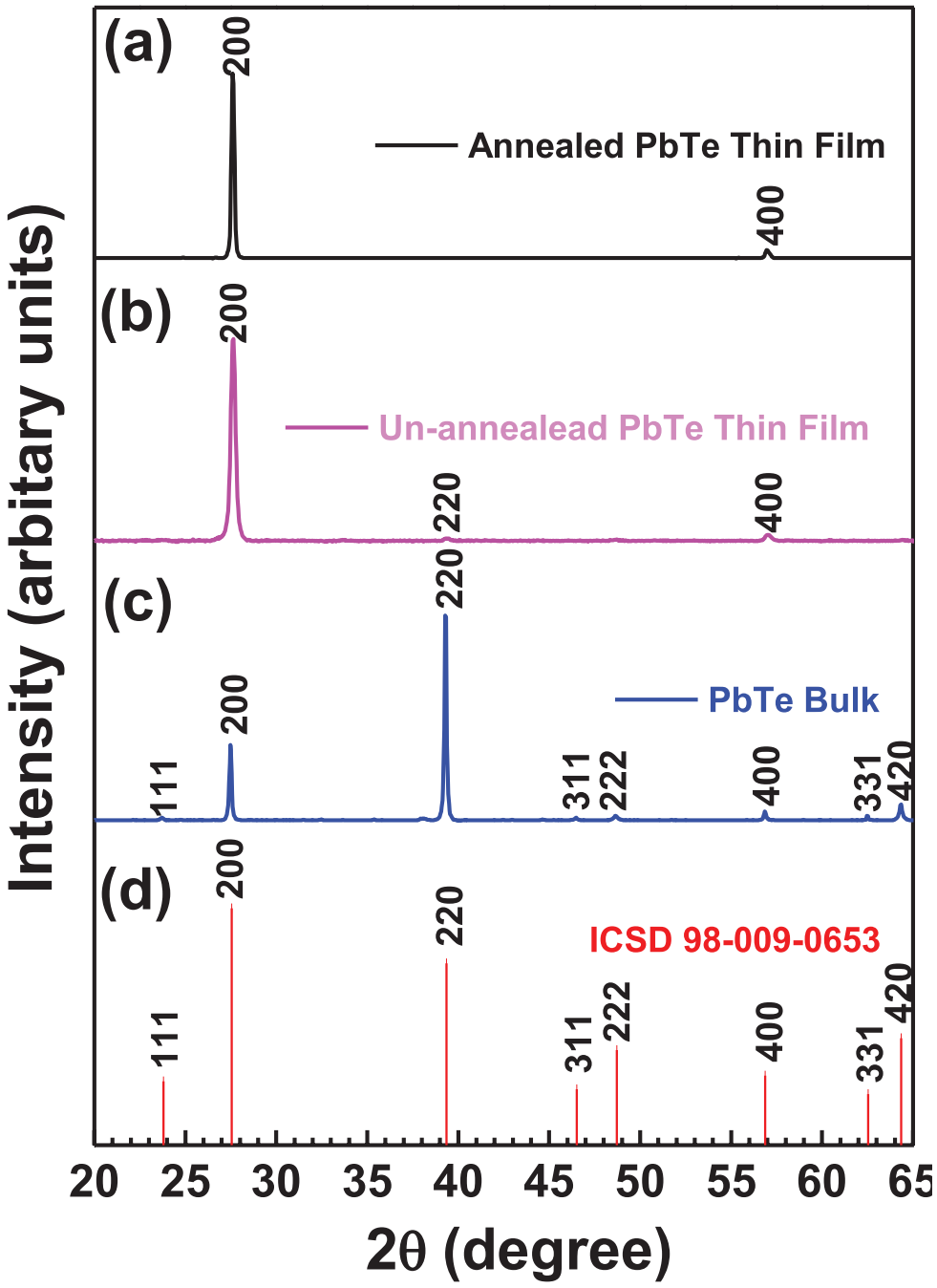

FIG. 1. XRD patterns of PbTe for (a) annealed thin film, (b) unannealed thin film, (c) bulk and (d) reference.

been reported yet. In this paper we present structural, electronic transport and MR measurements of a single crystal PbTe NW.

II. EXPERIMENTAL

PbTe NWs were synthesized using stress-induced growth, which is a practical method for growing NWs with a high aspect ratio and high crystallinity.[15] As-received Pb (Alfa Aesar, -200 mesh, 99.9%) and Te (Alfa Aesar, -325 mesh, 99.99%) powders were first mixed at

All article content, except where otherwise noted, is licensed under a Creative Commons Attribution 3.0 Unported license. See: http://creativecommons.org/licenses/by/3.0/
Downloaded to IP: 140.109.103.227 On: Wed, 14 May 2014 02:53:04

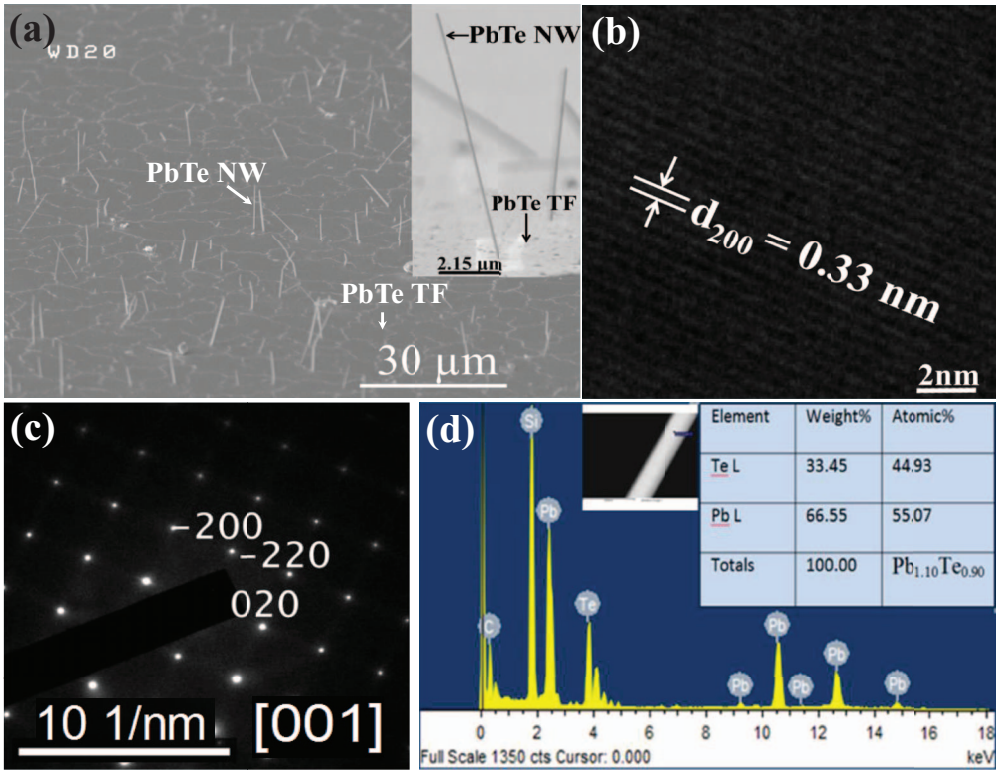

FIG. 2. (a) SEM image (top view) of the PbTe NWs grown from the surface of the PbTe thin film. (b) The distance between the crystal faces is 0.33 nm, indicating the growth direction along [200]. (c) The SAED pattern at the [001] zone axis. (d) EDS spectrum of a PbTe NW.

a specific ratio 1:1, and melted at 1000 °C for 4 h in a vacuumed quartz tube below 5 × 10^{-6} Torr. The molten compound was slowly cooled to room temperature in the furnace. Subsequently, a disk cut from the compound was served as the target for the pulsed laser deposition. Single-crystal SiO_2/Si (100) wafers (e-light Tech. Inc.; SiO_2 thickness, 413–434 nm; diameter, 100 ± 0.5 mm) with double-side polishing were cut into 1.5 × 1.5 cm^2 squares as substrates, which were cleaned using acetone, isopropyl alcohol, and deionized water in an ultrasonic bath for 10 min before being dried with N_2 stream. The PbTe films were prepared in an ArF excimer laser (Lamda Physik LPXpro 210) and deposited onto substrates in a vacuum system with a base pressure of 5.0 × 10^{-7} Torr. The PbTe thin films were grown with deposition rate at 0.22 Å/s, which the excimer laser was applied at 140 mJ (frequency, 10 Hz) for 15 min at room temperature. The substrate was rotated at approximately 10 rpm, and the thickness of the films was 20 nm. The films were sealed in a vacuumed quartz tube below 5 × 10^{-6} Torr, annealed at 450 °C for 5 d followed by furnace cool to room temperature. During the annealing process, the NWs were grown from the film by compressive stress release due to the difference of the thermal expansion coefficient between the PbTe film and SiO_2/Si substrate.

III. RESULTS AND DISCUSSIONS

Figures 1(a)–1(c) respectively show the X-ray diffraction (XRD) patterns of the PbTe for annealed thin film, un-annealed thin film and bulk. XRD spectra analysis was conducted for phase identification using a powder XRD (X'Pert PRO-PANalytical, CuKα radiation) from $2\theta = 20°$ to 65°. The Figures 1(a) and 1(b) show that the preferential orientation (h00) of a PbTe film. All of the diffraction peaks were indexed to the face-centered cubic (FCC) PbTe structure with the space group Fm-3m (225), as referenced from ICSD no. 98-009-0653 (Fig. 1(d)). With these data, the values of

All article content, except where otherwise noted, is licensed under a Creative Commons Attribution 3.0 Unported license. See: http://creativecommons.org/licenses/by/3.0/
Downloaded to IP: 140.109.103.227 On: Wed, 14 May 2014 02:53:04

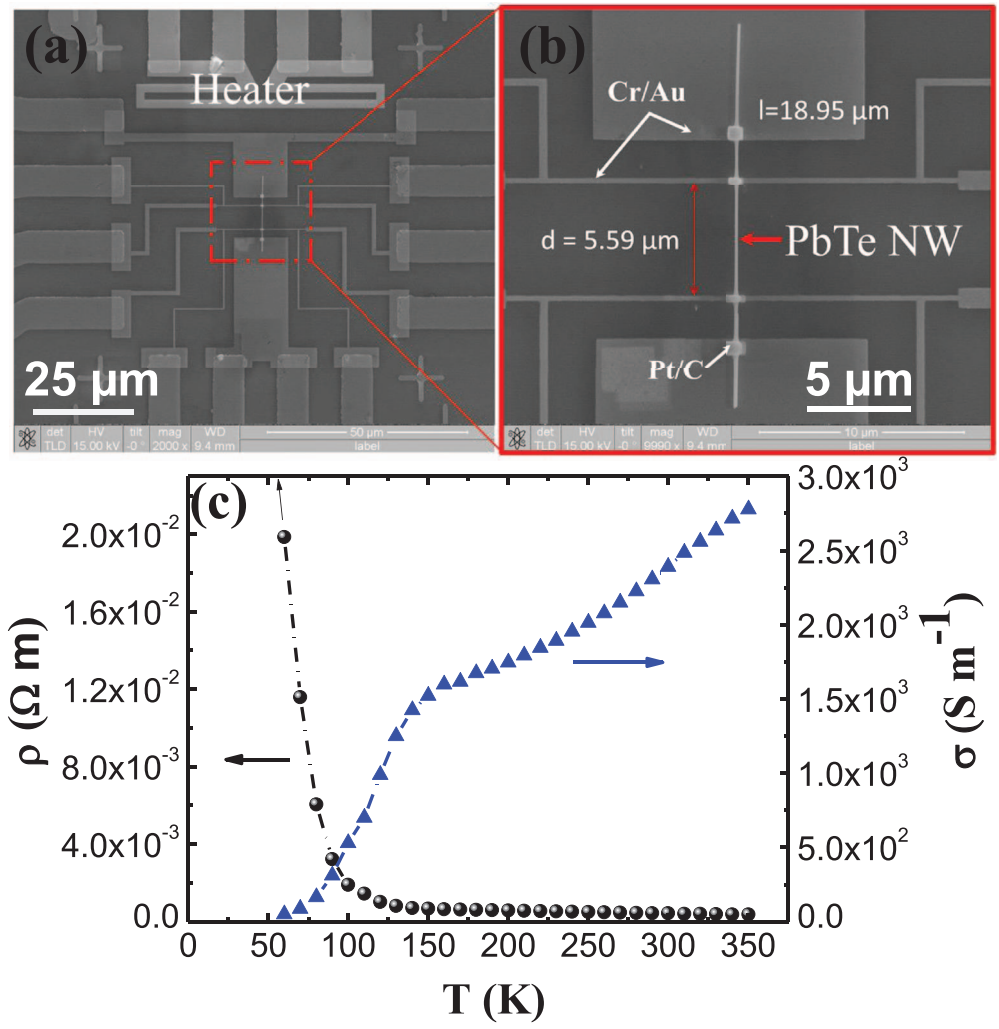

FIG. 3. (a)–(b) SEM images of a single-crystal PbTe NW (d = 142 nm, L = 18.95 μm) placed on a Si_3N_4 microchip following electrode formation using an FIB. (c) Temperature dependence of electrical resistivity and conductivity of the PbTe NW.

the PbTe lattice parameter a (using the Rietveld refinement program) were 6.46, 6.46, and 6.43 Å for the bulk, un-annealed and annealed films, respectively.

Straight and uniform PbTe NWs with a high aspect ratio grown on the substrate after annealing. Field emission scanning electron microscopy (FESEM; Hitachi, S-4800) images of the PbTe NWs (Fig. 2(a)) show the diameters of NWs ranging from 50 to 300 nm, and lengths up to 70 micrometers. A transmission electron microscope (TEM; JEOL JEM-2100 at 200 kV) was used to examine the crystalline structure of the PbTe NW. The TEM image shows that the lattice fringes of the PbTe NW are separated by a 0.33 nm gap which is consistent with a periodicity along the [200] direction with the lattice parameter a of 6.549 Å (Fig. 2(b)). A corresponding selected-area electron diffraction (SAED) pattern shows that the PbTe NWs are high-quality single crystals with growth direction along [100] (Fig. 2(c)). Typical energy dispersive x-ray spectroscopy (EDS) shows pronounced Pb and Te peaks, indicating the composition unaltered (Fig. 2(d)).

A tungsten needle (d = 100 nm) and a binocular optical microscope were used to extract a single-crystal NW from the PbTe thin film, it was then suspended on a Si_3N_4 microchip (Figs. 3(a) and 3(b)) for the measurements of electrical resistivity ρ and MR from 50 to 350 K using four-point

All article content, except where otherwise noted, is licensed under a Creative Commons Attribution 3.0 Unported license. See: http://creativecommons.org/licenses/by/3.0/
Downloaded to IP: 140.109.103.227 On: Wed, 14 May 2014 02:53:04

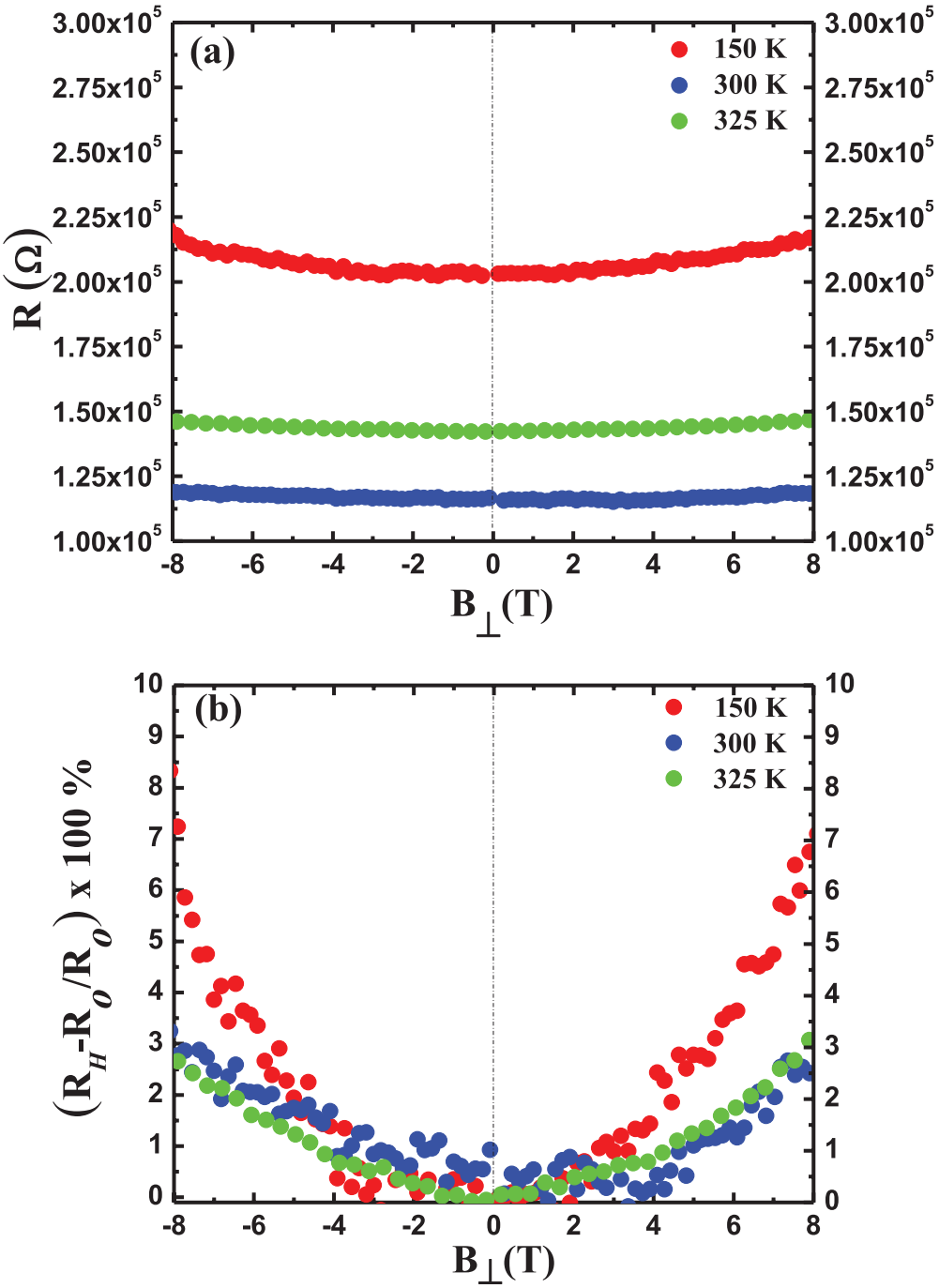

FIG. 4. (a) Electrical resistance and (b) magnetoresistance of the PbTe NW (d = 142 nm) as a function of the magnetic field at 325 K (green dot), 300 K (blue dot), and 150 K (red dot).

measurements. Figure 3(c) shows the temperature dependence of ρ and σ for a 142-nm NW that exhibits a semiconducting behavior.

The σ at near room temperature was 2383 S m^{-1}, which was lower than that of the PbTe bulk (65789.47 S m^{-1}).[8] It is likely caused by the difference in the carrier concentration or mobilities values. However, the value is higher than those reported in previous studies of NWs (σ = 0.44 – 1526 S m^{-1}).[15–17]

All article content, except where otherwise noted, is licensed under a Creative Commons Attribution 3.0 Unported license. See: http://creativecommons.org/licenses/by/3.0/
Downloaded to IP: 140.109.103.227 On: Wed, 14 May 2014 02:53:04

The MR was measured with the applied magnetic field B perpendicular to the longitudinal axis. In this arrangement, the electric current was perpendicular to B. The value of MR was calculated using the formula $MR = \frac{R_H - R_0}{R_0} \times 100\,\%$, where R_H and R_0 represent the resistance R with and without a magnetic field, respectively (Figs. 4(a) and 4(b)). The dependence of perpendicular MR up to B = ± 8 T of the 142 nm NW is parabolic for all measurement temperatures. The obtained positive MR for the 142-nm NW at 150 K is approximately 7% at B = 8 T, which is about 2.24 times higher than that at room temperature, whereas the room temperature MR of the 142 nm NW is ∼0.8% at B = 2 T, which is considerably higher than that of the PbTe bulk reported (MR = 0.2% at B = 2 T).[18] For the measurement at 325 K, the MR curve exhibits relatively similar behaviour to that of the measurement at 300 K. According to Al'tshuler *et al.*,[19] the sign and magnitude of MR and the temperature and field dependence characteristics of semiconductors are determined by multiple factors, including band structure, spin- and inter-valley relaxation mechanisms, sample dimensionality, interactions between impurities and electrons, and the scattering of electrons within the wire boundaries.

IV. SUMMARY

This study reports the structural characteristics *of a* single-crystal PbTe NW with 142-nm diameter that was synthesized using stress-induced growth. The NW exhibited semiconducting behavior and the electrical conductivity at near room temperature is 2383 S m^{-1}, which is higher than those reported in previous studies for single-crystal PbTe NW (σ = 0.44–1526 S m^{-1}).[15–17] Furthermore the magnetoresistance of the NW at 150 K was approximately 7% when the applied magnetic field was ± 8 T perpendiculars to the longitudinal axis, which was 2.24 times higher than that obtained at room temperature. No previous magnetoresistance study has reported this result for single-crystal PbTe NW.

ACKNOWLEDGMENTS

Technical support was provided by the Core Facilities for Nanoscience and Nanotechnology at the Institute of Physics, Academia Sinica in Taiwan. This work was supported by the National Science Council in Taiwan, under Grant No. NSC 100-2112-M-001-019-MY3.

[1] G. Springholz, T. Schwarzl, M. Aigle, H. Pascher, and W. Heiss, Appl. Phys. Lett. **76**, 1807 (2000).
[2] T. Schwarzl, W. Heiss, G. Springholz, M. Aigle, and H. Pascher, Electron. Lett. **36**, 322 (2000).
[3] S. M. Sze and K. K. Ng, *Physics of Semiconductor Devices*, 3rd ed. (Wiley-Interscience, Hoboken, NJ, 2007).
[4] C. Boschetti, I. Bandeira, H. Closs, A. Ueta, P. Rappl, P. Motisuke, and E. Abramof, Infrared Phys. Technol. **42**, 91 (2001).
[5] A. Barros, E. Abramof, and P. Rappl, J. Appl. Phys. **99**, 024904 (2006).
[6] Z. Dughaish, Phys. B - Cond. Matt. **322**, 205 (2002).
[7] J. P. Heremans, C. Thrush, and D. T. Morelli, Phys. Rev. B **70**, 115334 (2004).
[8] J. P. Heremans, C. Thrush, and D. T. Morelli, J. Appl. Phys. **98**, 063703 (2005).
[9] N. Romčević, J. Trajić, M. Romčević, D. Stojanović, T. A. Kuznetsova, D. R. Khokhlov, W. D. Dobrowolski, Optoele. and Adv. Mat. – Rap. Comm. **4**(4), 470 (2010).
[10] B. A. Volkov, L. I. Ryabova, and D. R. Khokhlov, Phys. Usp. **45**(8), 819 (2002).
[11] K. Lee, S. Lee, S. N. Holmes, J. Ham, W. Lee, and C. H. W. Barnes, Phys. Rev. B **82**, 245310 (2010).
[12] W. Shim, J. Ham, J. Kim, and W. Lee, Appl. Phys. Lett. **95**, 232107 (2009).
[13] J. Heremans, C. M. Thrush, Z. Zhang, X. Sun, M. S. Dresselhaus, J. Y. Ying, and D. T. Morelli, Phys. Rev. B. Rapid Comm. **58**, R10091 (1998).
[14] J. Heremans, C. M. Thrush, Y. M. Lin, S. Cronin, Z. Zhang, M. S. Dresselhaus, and J. F. Mansfield, Phys. Rev. B **61**, 2921 (2000).
[15] Dedi, P. C. Lee, C. H. Chien, G. P. Dong, W. C. Huang, C. L. Chen, C. M. Tseng, S. R. Harutyunyan, C. H. Lee, and Y. Y. Chen, Appl. Phys. Lett. **103**, p023115 (2013).
[16] S. Y. Jang, H. S. Kim, J. Park, M. Jung, J. Kim, S. H. Lee, J. W. Roh, and W. Lee, Nanotechnology **20**, 415204 (2009).
[17] G. Tai, B. Zhou, and W. Guo, J. Phys. Chem. C, **112**, 11314 (2008).
[18] V. V. Shchennikov and S. V. Ovsyannikov, Sol. State Comm. **126**, 373–378 (2003).
[19] B. L. Al'tshuler, A. G. Aronov, A. I. Larkin, and D. E. Khmel'nitskii, Sov. Phys. JETP **54**(2), 411 (1981).

All article content, except where otherwise noted, is licensed under a Creative Commons Attribution 3.0 Unported license. See: http://creativecommons.org/licenses/by/3.0/
Downloaded to IP: 140.109.103.227 On: Wed, 14 May 2014 02:53:04